Available online at www.sciencedirect.com
SCIENCE DIRECT®
International Journal of Heat and Mass Transfer 49 (2006) 3016–3027
International Journal of HEAT and MASS TRANSFER
www.elsevier.com/locate/ijhmt

Natural convection in a concentric annulus with a porous sleeve

J.C. Leong [a], F.C. Lai [b,*]

[a] Department of Vehicle Engineering, National Pingtung University of Science and Technology, Pingtung, Taiwan
[b] School of Aerospace and Mechanical Engineering, University of Oklahoma, 865 Asp Avenue, Norman, OK 73019-0601, USA

Received 1 June 2005; received in revised form 27 January 2006
Available online 17 April 2006

Abstract

Analytical solutions obtained through perturbation method and Fourier transform are presented for natural convection in concentric cylinders with a porous sleeve. The porous sleeve is press-fitted to the inner surface of the outer cylinder. Both the inner and outer cylinders are kept at constant temperatures with the inner surface at a slightly higher temperature than that of the outer. The main objective of the present study is to investigate the buoyancy-induced flow as affected by the presence of the porous layer. A parametric study has been performed to investigate the effects of Rayleigh number, Darcy number, porous sleeve thickness, and relative thermal conductivity on the heat transfer results.

1. Introduction

Natural convection in horizontal annuli has long been a subject of engineering interest. Earlier work includes several experimental studies with flow visualization by Bishop and Carley [1] and Powe et al. [2,3]. Kuehn and Goldstein [4,5] examined this problem from both experimental and numerical perspectives. Charrier-Mojtabi et al. [6], on the other hand, performed a numerical study on the same subject. Since then, this problem has been extended to include the effect of eccentricity [7–11] and to the field of porous media [12–14]. Caltagirone [12] studied natural convection in a saturated porous medium bounded by two horizontal concentric cylinders. Later, Bau [13] examined natural convection in an eccentric porous annulus at low Rayleigh numbers using the perturbation method.

The present work examines the flow and temperature fields in a concentric annulus with a porous sleeve. Different from the previous studies mentioned above, the present study considers a fluid layer and a porous layer of finite thickness. In fact, the study of flow interaction between a fluid and a porous layer can be dated back to the sixties. Ishizawa and Hori [14] had obtained the normal velocity profiles of a viscous fluid through a porous wall into a narrow gap. For applications, a horizontal annulus with a porous sleeve is of practical interest. For example, heat transfer in an annulus with scale or ice slurry developed on the inner surface of the outer cylinder is important for heat exchanger design. Another related application is the use of porous bearings in rotary machinery.

2. Formulation and numerical method

The physical configuration of the present study (Fig. 1) consists of two infinitely long cylinders of radii a and c. They are maintained at constant temperatures, T_H (on the inner cylinder) and T_L (on the outer cylinder) with $T_H > T_L$. In between, a porous sleeve of inner radius b is press-fitted to the inner surface of the outer cylinder. Thus, the configuration consists of an inner fluid region and an outer porous region. It is assumed that the porous matrix is homogeneous, isotropic and saturated with the same fluid in the fluid region. The effects of temperature on the fluid and porous matrix properties other than density are assumed negligible due to the small temperature difference. Since both

* Corresponding author. Tel.: +1 405 325 1748; fax: +1 405 325 1088.
E-mail address: flai@ou.edu (F.C. Lai).

0017-9310/$ - see front matter © 2006 Elsevier Ltd. All rights reserved.
doi:10.1016/j.ijheatmasstransfer.2006.01.039

Nomenclature

a	radius of the inner cylinder (m)
b	inner radius of the porous sleeve (m)
c	radius of the outer cylinder (m)
c_p	heat capacity (J/kg K)
Da	Darcy number, $Da = K/b^2$
g	gravitational acceleration (m/s^2)
K	permeability (m^2)
k	effective thermal conductivity of porous medium (W/m K)
Nu	Nusselt number, $Nu = hb/k$
$\overline{Nu}$	average Nusselt number
P	pressure (Pa)
Pr	Prandtl number, $Pr = \nu/\alpha_1$
R	normalized radial distance in cylindrical coordinate system, $R = r/b$
r	radial distance in cylindrical coordinate system (m)
Ra	Rayleigh number, $Ra = g\beta(T_H - T_L)b^3/\nu\alpha_1$
T	temperature (K)
u_r, u_θ	velocity components in cylindrical coordinate system (m/s)

Greek symbols

α	thermal diffusivity, $k/\rho c_p$ (m^2/s)
β	coefficient of thermal expansion (1/K)
μ	dynamic viscosity of fluid (kg/m s)
$\tilde{\mu}$	effective viscosity in Brinkman model (kg/m s)
ν	kinematic viscosity of fluid (m^2/s)
ρ	fluid density (kg/m^3)
Θ	normalized temperature, $\Theta = (T - T_L)/(T_H - T_L)$
θ	azimuthal angle in cylindrical coordinate system
Ψ	dimensionless stream function, $\Psi = \psi/\alpha_1$
ψ	stream function (m^2/s)

Subscripts

in	inner cylinder
out	outer cylinder
1	fluid layer
2	porous layer

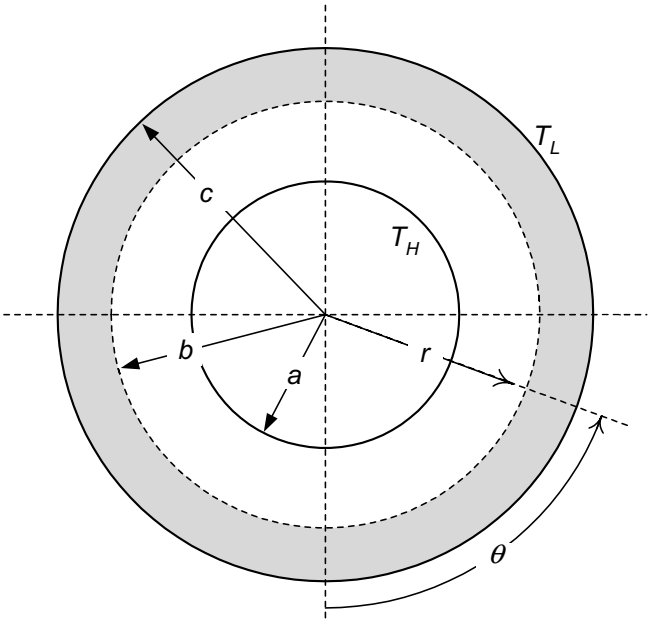

Fig. 1. A concentric annulus with a porous sleeve subject to differential heating from the inner and outer wall ($T_H > T_L$).

cylinders are stationary, the fluid motion is induced by the thermal buoyancy resulting from the differential heating between the cylinders. It is further assumed that the buoyancy-induced flow is steady and laminar.

The governing equations in terms of stream function and temperature for both fluid and porous layers are given by

$$\frac{1}{r}\left(\frac{\partial\psi_1}{\partial r}\frac{\partial\nabla^2\psi_1}{\partial\theta} - \frac{\partial\psi_1}{\partial\theta}\frac{\partial\nabla^2\psi_1}{\partial r}\right) = g\beta\left(\sin\theta\frac{\partial T_1}{\partial r} + \frac{\cos\theta}{r}\frac{\partial T_1}{\partial\theta}\right) + \nu\nabla^4\psi_1, \quad (1)$$

$$\frac{1}{r}\left(\frac{\partial\psi_1}{\partial r}\frac{\partial T_1}{\partial\theta} - \frac{\partial\psi_1}{\partial\theta}\frac{\partial T_1}{\partial r}\right) = \alpha_1\nabla^2 T_1, \quad (2)$$

$$\frac{\rho}{r}\left(\frac{\partial\psi_2}{\partial r}\frac{\partial\nabla^2\psi_2}{\partial\theta} - \frac{\partial\psi_2}{\partial\theta}\frac{\partial\nabla^2\psi_2}{\partial r}\right) = \rho g\beta\left(\sin\theta\frac{\partial T_2}{\partial r} + \frac{\cos\theta}{r}\frac{\partial T_2}{\partial\theta}\right) - \frac{\mu}{K}\nabla^2\psi_2 + \tilde{\mu}\nabla^4\psi_2, \quad (3)$$

$$\frac{1}{r}\left(\frac{\partial\psi_2}{\partial r}\frac{\partial T_2}{\partial\theta} - \frac{\partial\psi_2}{\partial\theta}\frac{\partial T_2}{\partial r}\right) = \alpha_2\nabla^2 T_2, \quad (4)$$

where subscripts 1 and 2 refer to the fluid region and porous layer, respectively. ∇ is the regular Laplacian operator and is given by

$$\nabla^2 = \frac{\partial^2}{\partial r^2} + \frac{1}{r}\frac{\partial}{\partial r} + \frac{1}{r^2}\frac{\partial^2}{\partial\theta^2}. \quad (5)$$

For the fluid region, Eqs. (1) and (2) are exactly the same as those derived by Yao [7]. For the porous layer, Eqs. (3) and (4) are formulated using the Brinkman extended Darcy law. The governing equations are normalized to give

$$\frac{1}{Pr}\frac{1}{R}\left(\frac{\partial\Psi_1}{\partial R}\frac{\partial\overline{\nabla}^2\Psi_1}{\partial\theta} - \frac{\partial\Psi_1}{\partial\theta}\frac{\partial\overline{\nabla}^2\Psi_1}{\partial R}\right) = Ra\left(\sin\theta\frac{\partial\Theta_1}{\partial R} + \frac{\cos\theta}{R}\frac{\partial\Theta_1}{\partial\theta}\right) + \overline{\nabla}^4\Psi_1, \quad (6)$$

$$\frac{1}{R}\left(\frac{\partial \Psi_1}{\partial R}\frac{\partial \Theta_1}{\partial \theta}-\frac{\partial \Psi_1}{\partial \theta}\frac{\partial \Theta_1}{\partial R}\right)=\overline{\nabla}^2\Theta_1, \tag{7}$$

$$\frac{1}{Pr}\frac{1}{R}\left(\frac{\partial \Psi_2}{\partial R}\frac{\partial \overline{\nabla}^2\Psi_2}{\partial \theta}-\frac{\partial \Psi_2}{\partial \theta}\frac{\partial \overline{\nabla}^2\Psi_2}{\partial R}\right) = Ra\left(\sin\theta\frac{\partial \Theta_2}{\partial R}+\frac{\cos\theta}{R}\frac{\partial \Theta_2}{\partial \theta}\right)-\frac{1}{Da}\overline{\nabla}^2\Psi_2+\overline{\nabla}^4\Psi_2, \tag{8}$$

$$\frac{\alpha_1}{R}\left(\frac{\partial \Psi_2}{\partial R}\frac{\partial \Theta_2}{\partial \theta}-\frac{\partial \Psi_2}{\partial \theta}\frac{\partial \Theta_2}{\partial R}\right)=\alpha_2\overline{\nabla}^2\Theta_2, \tag{9}$$

where the normalized Laplacian operator is given by

$$\overline{\nabla}^2=\frac{\partial^2}{\partial R^2}+\frac{1}{R}\frac{\partial}{\partial R}+\frac{1}{R^2}\frac{\partial^2}{\partial \theta^2}=b^2\nabla^2. \tag{10}$$

The corresponding boundary and interface conditions are given below.

On the surface of the inner cylinder,

$$r=a,\quad u_{r1}=0,\quad u_{\theta 1}=0,\quad T_1=T_{\mathrm{H}}. \tag{11a}$$

On the surface of the outer cylinder,

$$r=c,\quad u_{r2}=0,\quad u_{\theta 2}=0,\quad T_2=T_{\mathrm{L}}. \tag{11b}$$

On the interface between the fluid layer and the porous sleeve,

$$r=b,\quad u_{r1}=u_{r2},\quad u_{\theta 1}=u_{\theta 2}, \tag{11c}$$

$$\mu_1\frac{\partial u_{\theta 1}}{\partial r}=\mu_2\frac{\partial u_{\theta 2}}{\partial r},\quad P_1=P_2, \tag{11d}$$

$$T_1=T_2,\quad k_1\frac{\partial T_1}{\partial r}=k_2\frac{\partial T_2}{\partial r}. \tag{11e}$$

In the dimensionless form, they are given by

$$\text{At } R=a/b,\quad \frac{\partial \Psi_1}{\partial \theta}=0,\quad \frac{\partial \Psi_1}{\partial R}=0,\quad \Theta_1=1. \tag{12a}$$

$$\text{At } R=c/b,\quad \frac{\partial \Psi_2}{\partial \theta}=0,\quad \frac{\partial \Psi_2}{\partial R}=0,\quad \Theta_2=0. \tag{12b}$$

$$\text{At } R=1,\quad \frac{\partial \Psi_1}{\partial \theta}=\frac{\partial \Psi_2}{\partial \theta},\quad \frac{\partial \Psi_1}{\partial R}=\frac{\partial \Psi_2}{\partial R}. \tag{12c}$$

$$\overline{\nabla}^2\Psi_1=\overline{\nabla}^2\Psi_2,\quad \frac{\partial \overline{\nabla}^2\Psi_1}{\partial R}=\frac{\partial \overline{\nabla}^2\Psi_2}{\partial R}-\frac{1}{Da}\frac{\partial \Psi_2}{\partial R}, \tag{12d}$$

$$\Theta_1=\Theta_2,\quad \frac{\partial \Theta_1}{\partial R}=\frac{k_2}{k_1}\frac{\partial \Theta_2}{\partial R}. \tag{12e}$$

3. Solution method

Since the temperature difference between the cylinders is small, the corresponding Rayleigh number is also small. For the present study, the solutions are obtained using the perturbation method. Although a direct numerical solution of the problem is possible, analytical solution is preferred here. Particularly, the closed form solutions obtained from the present study are intended for code validation for a related study [15]. In the spirit of perturbation method, the solutions for the stream function and temperature are sought in the form of power series of the Rayleigh number

$$\Psi_1=\Psi_{10}+Ra\Psi_{11}+Ra^2\Psi_{12}+\cdots, \tag{13a}$$

$$\Theta_1=\Theta_{10}+Ra\Theta_{11}+\cdots, \tag{13b}$$

$$\Psi_2=\Psi_{20}+Ra\Psi_{21}+Ra^2\Psi_{22}+\cdots, \tag{14a}$$

$$\Theta_2=\Theta_{20}+Ra\Theta_{21}+\cdots. \tag{14b}$$

Analytical solutions up to the second leading terms are obtained and presented in this paper. Substitute the above solution forms to their governing equations as well as the boundary and interface conditions, respectively. After collecting the terms with the same power of the Rayleigh number, one obtains four sets of governing equations and their corresponding boundary and interface conditions at different solution levels (orders). For brevity, the formulations of these subset problems are not presented here but can be found in Ref. [16].

To solve the problems at various levels, Finite Fourier Transform is used in which the independent variable θ is transformed to a parameter σ. Osizik [17] has successfully demonstrated the use of this transform in classical heat conduction problems. In the present work, there is no prescribed boundary condition for the independent variable θ except the requirement that the flow and temperature fields have to be continuous around the annulus with a period of 2π. This transformation is performed as follows:

Fourier transform

$$\bar{\Phi}(r,n,\sigma)=\overline{F}\{\Phi(r,\tilde{\sigma})\}=\int_0^{2\pi}\cos n(\sigma-\tilde{\sigma})\times\Phi(r,\tilde{\sigma})\times \mathrm{d}\tilde{\sigma}. \tag{15a}$$

Inverse transform

$$\Phi(r,\sigma)=\frac{1}{2\pi}\bar{\Phi}(r,0,\sigma)+\frac{1}{\pi}\sum_{n=1}^{\infty}\bar{\Phi}(r,n,\sigma)\Phi(r,\sigma) =\frac{1}{2\pi}\bar{\Phi}(r,0,\sigma)+\frac{1}{\pi}\sum_{n=1}^{\infty}\bar{\Phi}(r,n,\sigma). \tag{15b}$$

Solving the problems in a sequential manner at the corresponding powers of the Rayleigh number, one obtains the following solutions:

$$\Psi_{10}=0, \tag{16a}$$

$$\Psi_{21}=0, \tag{16b}$$

$$\Theta_{10}=\frac{(k_1/k_2)\ln(c/b)-\ln(R)}{(k_1/k_2)\ln(c/b)-\ln(a/b)}, \tag{17a}$$

$$\Theta_{20}=\frac{(k_1/k_2)\ln(c/b)-(k_1/k_2)\ln(R)}{(k_1/k_2)\ln(c/b)-\ln(a/b)}, \tag{17b}$$

$$\Psi_{11}=\frac{A_{11}}{8}R^3+\frac{B_{11}}{2}R\ln(R)+C_{11}R+D_{11}R^{-1}+\left(\frac{\ln(R)}{8}-\frac{3}{32}\right)\Gamma_{11}R^3, \tag{18a}$$

$$\Psi_{21}=\frac{A_{21}}{\gamma^2}I_1(\gamma R)+\frac{B_{21}}{\gamma^2}K_1(\gamma R)+C_{21}R+D_{21}R^{-1}+\frac{\Gamma_{21}}{2}R\ln(R), \tag{18b}$$

$$\Theta_{11} = q\left[\frac{A'_{11}}{64}R^3 + \frac{\ln(R)^2 - \ln(R)}{8}B'_{11}R + \frac{C'_{11}}{2}R\ln(R) - \frac{D'_{11}}{2}\frac{\ln(R)}{R} + E_{11}R + F_{11}R^{-1} + \left(\frac{\ln(R)}{64} - \frac{3}{128}\right)\Gamma'_{11}R^3\right], \tag{19a}$$

$$\Theta_{21} = q\left(\frac{k_1}{k_2}\right)^2\left[\frac{A'_{21}}{\gamma^3}R\int_1^R \frac{I_0(\gamma\xi)}{\xi^3}\mathrm{d}\xi - \frac{B'_{21}}{\gamma^3}R\int_1^R \frac{K_0(\gamma\xi)}{\xi^3}\mathrm{d}\xi + \frac{C'_{21}}{2}R\ln(R) - \frac{D'_{21}}{2}\frac{\ln(R)}{R} + E_{21}R + F_{21}R^{-1} + \frac{\ln(R)^2 - \ln(R)}{8}\Gamma'_{21}R\right], \tag{19b}$$

$$\Psi_{12} = \frac{X_1}{384}R^6\ln(R)^2 + \left(-\frac{25X_1}{4608} + \frac{X_2}{384}\right)R^6\ln(R) + \left(\frac{415X_1}{110592} - \frac{25X_2}{9216} + \frac{X_3}{384}\right)R^6 + \frac{X_4}{144}R^4\ln(R)^3 + \left(-\frac{11X_4}{576} + \frac{X_5}{96}\right)R^4\ln(R)^2 + \left(\frac{85X_4}{3456} - \frac{11X_5}{576} + \frac{X_6}{48}\right)R^4\ln(R) + \left(-\frac{137X_4}{10368} + \frac{19X_5}{1728} - \frac{X_6}{72} + \frac{A_{12}}{12}\right)R^4 - \frac{X_7}{32}R^2\ln(R)^2 + \left(\frac{X_7}{64} - \frac{X_8}{16}\right)R^2\ln(R) + C_{12}R^2 + \frac{X_9}{16}\ln(R) - \frac{B_{12}}{4} + D_{12}R^{-2}, \tag{20a}$$

$$\Psi_{22} = C_{22}R^2 + D_{22}R^{-2} + \frac{R^2}{4}\int_1^R \frac{W(\xi)}{\xi}\mathrm{d}\xi - \frac{R^{-2}}{4}\int_1^R \xi^3 W(\xi)\mathrm{d}\xi. \tag{20b}$$

Notice that the functions I and K in the above equations are the modified Bessel functions of the first and second kinds, respectively. The prime denotes the partial derivative with respect to R. The coefficients in each equation are listed in Appendix A. Clearly, Θ_{10} and Θ_{20} represent the solutions of conduction for the limiting case of $Ra = 0$. As such, there is no flow inside the annulus (Eqs. (16a) and (16b)).

The heat transfer results are evaluated in terms of the Nusselt number on both inner and outer cylinders. By definition, the local Nusselt numbers represent the local heat flux and are given by

$$Nu_{\mathrm{in}} = \frac{hb}{k_1} = -\frac{\partial\Theta_1}{\partial R} \tag{21a}$$

and

$$Nu_{\mathrm{out}} = \frac{hb}{k_2} = -\frac{\partial\Theta_2}{\partial R}. \tag{21b}$$

To evaluate the average Nusselt number, one integrates the local Nusselt number over the circumference of the cylinder

$$\overline{Nu}_{\mathrm{in}} = \frac{q}{a/b} - Ra\frac{q}{\pi}\int_0^\pi \widetilde{\Theta}'_{11}\big|_{R=a/b}\mathrm{d}\theta + \cdots, \tag{22a}$$

and

$$\overline{Nu}_{\mathrm{out}} = \frac{k_1}{k_2}\frac{q}{c/b} - Ra\frac{k_1}{k_2}\frac{q}{\pi}\int_0^\pi \tilde{\Theta}'_{21}\big|_{R=c/b}\mathrm{d}\theta + \cdots, \tag{22b}$$

where

$$\widetilde{\Theta}'_{11} = \frac{3R^2}{64}A'_{11} + \frac{\ln(R)^2 + \ln(R) - 1}{8}B'_{11} + \frac{\ln(R) + 1}{2}C'_{11} - \frac{\ln(R) - 1}{2R^2}D'_{11} + E_{11} - \frac{F_{11}}{R^2} + \frac{\Gamma'_{11}R^2}{64}\left(3\ln(R) - \frac{7}{2}\right), \tag{23a}$$

and

$$\widetilde{\Theta}'_{21} = \frac{A'_{21}}{\gamma^3}\left(\int_1^R \frac{I_0(\gamma\xi)}{\xi^3}\mathrm{d}\xi + \frac{I_0(\gamma R)}{R^2}\right) - \frac{B'_{21}}{\gamma^3}\left(\int_1^R \frac{K_0(\gamma\xi)}{\xi^3}\mathrm{d}\xi + \frac{K_0(\gamma R)}{R^2}\right) + \frac{C'_{21}}{2}[\ln(R) + 1] + \frac{D'_{21}}{2R^2}(\ln(R) - 1) + E_{21} - \frac{F_{21}}{R^2} + \frac{\Gamma'_{21}}{8}\left[\ln(R)^2 + \ln(R) - 1\right]. \tag{23b}$$

Since the temperature field is symmetrical about the vertical axis (and thus it is an even function), the limit of integration in Eqs. (22) is from 0 to π.

4. Results and discussion

The present study is focused on the effects of Rayleigh number, porous sleeve thickness, Darcy number, and the effective thermal conductivity ratio on the flow and temperature fields in a concentric annulus with a porous sleeve. Among the parameters considered, Rayleigh number signifies the thermal buoyancy induced by the differential heating between the inner and outer cylinders. Mathematically, a solution obtained by the perturbation method is valid only for a small perturbed quantity (Rayleigh number in the present study). However, in the literature, Mack and Bishop [18] have reported solutions for which the Rayleigh number is as high as 10^3. In a similar study, Huetz and Petit [19] as well as Custer and Shaughnessy [20] all have obtained converged solutions with the Grashof number (their perturbed quantity) in an order up to 10^4. The reason why the solution still converges at these values may be due to the fact that convection remains very weak in the range of these numbers. For the present study, it has been found that the flow and temperature fields as well as the heat transfer results predicted by the present analytical solutions agree very well with those of the direct numerical solutions for Rayleigh numbers up to 100. Typically, a Rayleigh number on the order of 100 corresponds to a temperature difference of 0.1 K for an annulus with a gap width of 1 cm. Therefore, the buoyancy-induced flow is small but finite.

For the discussion that follows, we limit our attention to a specific configuration of $a = 1$, $b = 1.5$, and $c = 2$, unless specified otherwise. Also, the flow and temperature fields are presented in the contour plots of stream function and isotherm, respectively.

Fig. 2 shows the effect of porous sleeve thickness on the flow and temperature fields at the Rayleigh number of unity. An increase in the value of b implies a reduction in the porous sleeve thickness. This can be clearly observed by the locations of the interface (dashed line) between the inner and outer cylinders. Apparently, the flow fields are symmetrical about the vertical diameter. On each side of the vertical diameter, there exists a convective cell. The left cell rotates in the counter-clockwise direction while the right cell of equal strength rotates in the clockwise direction. As the thickness of the porous sleeve reduces (i.e., b increases), the flow resistance in the entire annulus decreases accordingly. As a result, less energy is lost through the flow resistance and which leads to a stronger convective flow. In general, the eyes of the convective cells are located within the fluid layer. At $b = 1.75$, the porous sleeve is nearly impermeable and convection is mainly confined in the fluid layer. As b decreases, the convective cells penetrate the porous sleeve. At $b = 1.25$, the fluid layer is too thin to contain the convective cells. As such, the cells penetrate the porous sleeve and their strength decreases accordingly.

Also observed is that the isotherms appear to be a family of concentric circles and thus the temperature profiles are independent of the azimuthal angle. Regardless of the location of the interface, the spacing between isotherms remains little changed. This indicates that the sleeve thickness has nearly no effect on the temperature distribution. Because heat conduction is the dominant heat transfer mode in these cases, the isotherms are distributed in proportion to the logarithm of the radial distance. The result is consistent with the assumption made at the beginning of the study (that is, a small Rayleigh number). A small Rayleigh number implies that heat convection is insignificant, or in other words, heat conduction is the dominant heat transfer mode in the system. This observation is also consistent with the results of Kuehn and Goldstein [4]. They have shown that the critical Rayleigh number Ra_L for the onset of heat convection in concentric cylinders is about 10^3, where Ra_L is defined based on the gap width, L. Since the presence of a porous sleeve imposes additional resistance on the convective flow, it is reasonable to expect that the critical Rayleigh number for a concentric annulus with a porous sleeve would be higher than 10^3.

Presented in Fig. 3 are the flow and temperature fields at various Darcy numbers. A Darcy number with a unity value implies that the pore size in the porous sleeve is of the same order of magnitude as the gap width. This in turn signifies that the flow resistance in the porous sleeve is basically non-existent. As such, the flow structures for $Da = 10^{-1}$ resemble those with a porous sleeve that is highly permeable. As the Darcy number decreases, the flow resistance becomes more significant. It is more difficult for the convective flow to penetrate the porous sleeve, which leads to weaker convective cells. In addition, it is clearly observed that the eye of the convective cells moves inward as the Darcy number decreases. Since the flow penetration decreases with a reduction in the Darcy number, the cells are mostly confined in the fluid layer and thus the eyes

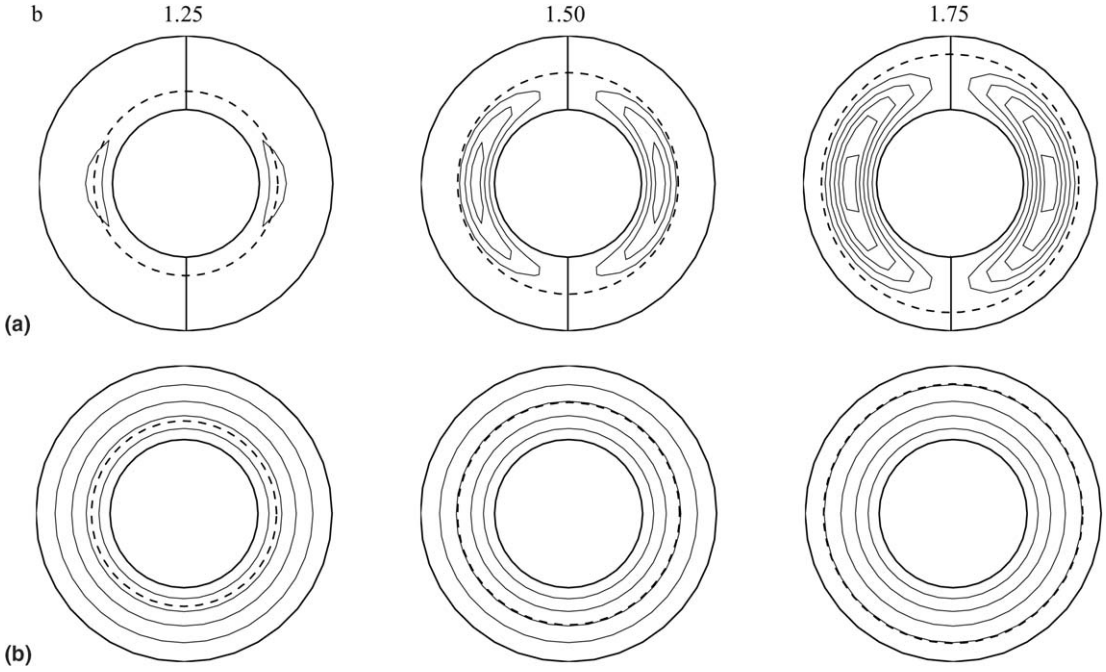

Fig. 2. Effect of porous sleeve thickness on natural convection in concentric cylinders with a porous sleeve for $Ra = 1$, $Da = 10^{-4}$, $k_1/k_2 = 1$, and $Pr = 2 \times 10^4$: (a) flow fields ($\Delta\Psi = 2 \times 10^{-5}$ for $b = 1.25$ and 1.5, $\Delta\Psi = 1 \times 10^{-4}$ for $b = 1.75$); (b) temperature fields ($\Delta\Theta = 0.2$).

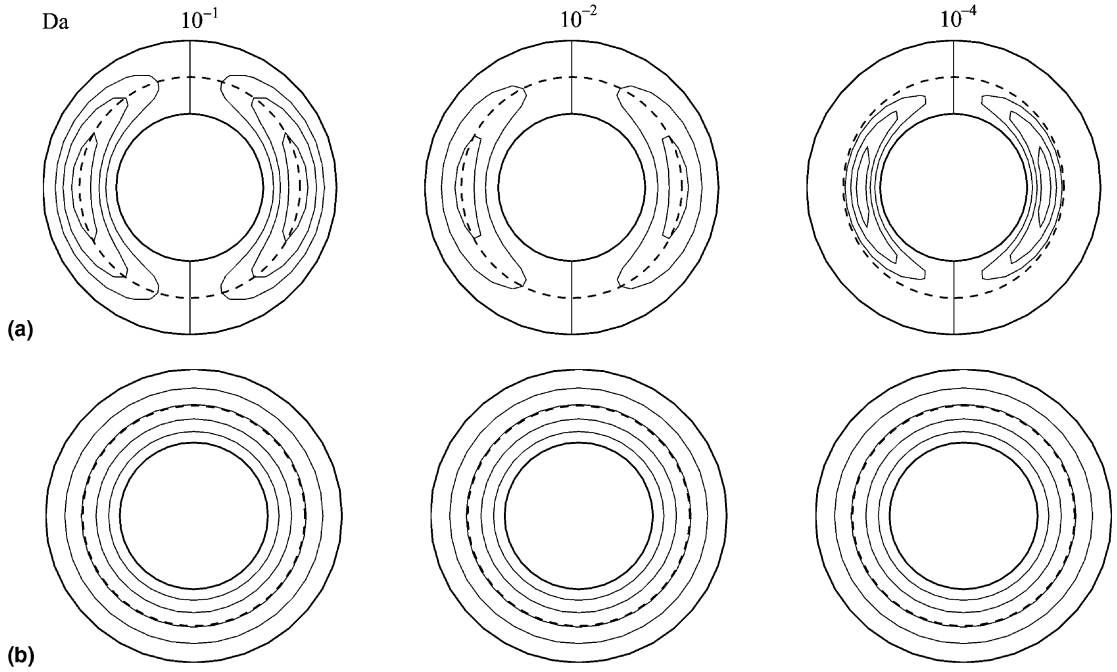

Fig. 3. Effect of Darcy number on natural convection in concentric cylinders with a porous sleeve for $Ra = 1$, $b = 1.5$, $k_1/k_2 = 1$, and $Pr = 2 \times 10^4$: (a) flow fields ($\Delta\Psi = 2 \times 10^{-4}$ for $Da = 10^{-1}$ and 10^{-2}, $\Delta\Psi = 2 \times 10^{-5}$ for $Da = 10^{-4}$); (b) temperature fields ($\Delta\Theta = 0.2$).

are pushed inward. Since the conductivity ratio is fixed at unity, the isotherm patterns are identical. This also shows that the temperature gradients are too small to induce significant heat convection.

The effects of thermal conductivity ratio k_1/k_2 are examined in Fig. 4. At a small Rayleigh number, the convective cells are confined within the fluid layer. Also noticed is that the convective cells become weaker with an increase in the thermal conductivity ratio. For $k_1/k_2 > 1$, the porous sleeve has a smaller thermal conductivity and thus leads to a larger temperature gradient in the porous sleeve to initiate convection and flow penetration. The figure also shows that the temperature fields depend mostly on the thermal conductivity ratio but not the Rayleigh number. Because

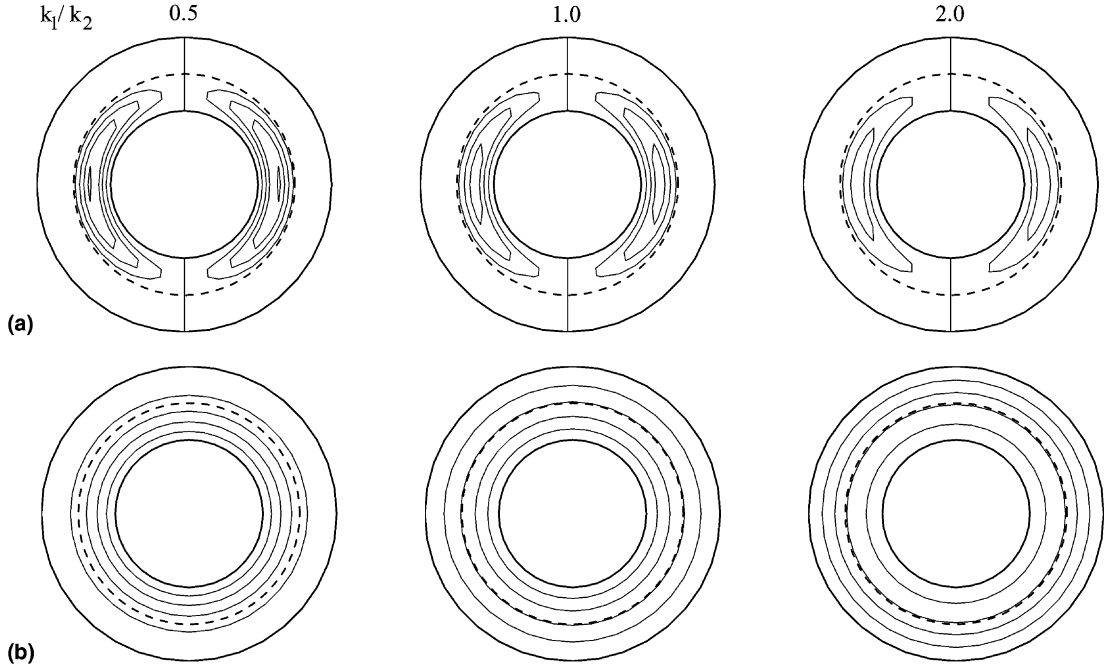

Fig. 4. Effect of thermal conductivity ratio on natural convection in concentric cylinders with a porous sleeve for $Ra = 1$, $Da = 10^{-4}$, $b = 1.5$, and $Pr = 2 \times 10^4$: (a) flow fields ($\Delta\Psi = 2 \times 10^{-5}$); (b) temperature fields ($\Delta\Theta = 0.2$).

heat conduction is the dominant heat transfer mode for these cases, the Rayleigh number only plays a minor role. When $k_1/k_2 = 1$, the isotherms are relatively evenly distributed within the gap because there is no distinction between the fluid and porous sleeve as far as heat conduction is concerned. For $k_1/k_2 < 1$, the porous sleeve is more conductive than the fluid layer. As a result, a large temperature gradient is found in the fluid layer while temperature is almost uniform in the porous sleeve. Conversely, for $k_1/k_2 > 1$, the temperature in the fluid layer is more uniform than that in the porous sleeve.

The combined effects of Darcy number and conductivity ratio can be examined from Figs. 5 and 6. As observed, the flow fields (Fig. 5) show a similar trend as that observed in Fig. 3. As the Darcy number decreases, the convective cell weakens in strength along with its eye moving toward the fluid layer. Notice that the increment of the stream function $\Delta\Psi$ for the case of $Da = 10^{-4}$ is only half of the other cases. Therefore, its strength is actually much weaker than it appears in the figure. When the porous sleeve is less permeable ($Da = 10^{-4}$), a smaller thermal conductivity ratio ($k_1/k_2 < 1$) leads to a larger temperature gradient in the fluid layer. A larger temperature gradient represents a stronger driving force to produce a more vigorous convective flow. As such, the strength of the convective flow decreases with an increase in the conductivity ratio. When the porous sleeve is considerably permeable ($Da = 10^0$ and 10^{-2}), the strength of the convective cells on the other hand grows with the thermal conductivity ratio k_1/k_2. Remember that, at this range of Darcy numbers, the flow in the annulus behaves as if it were in a single fluid layer. At $k_1/k_2 = 0.5$, a higher temperature gradient appears in the fluid layer, leaving the porous sleeve almost isothermal. As k_1/k_2 increases, the temperature gradient in the porous sleeve increases, leading to a stronger convective cell.

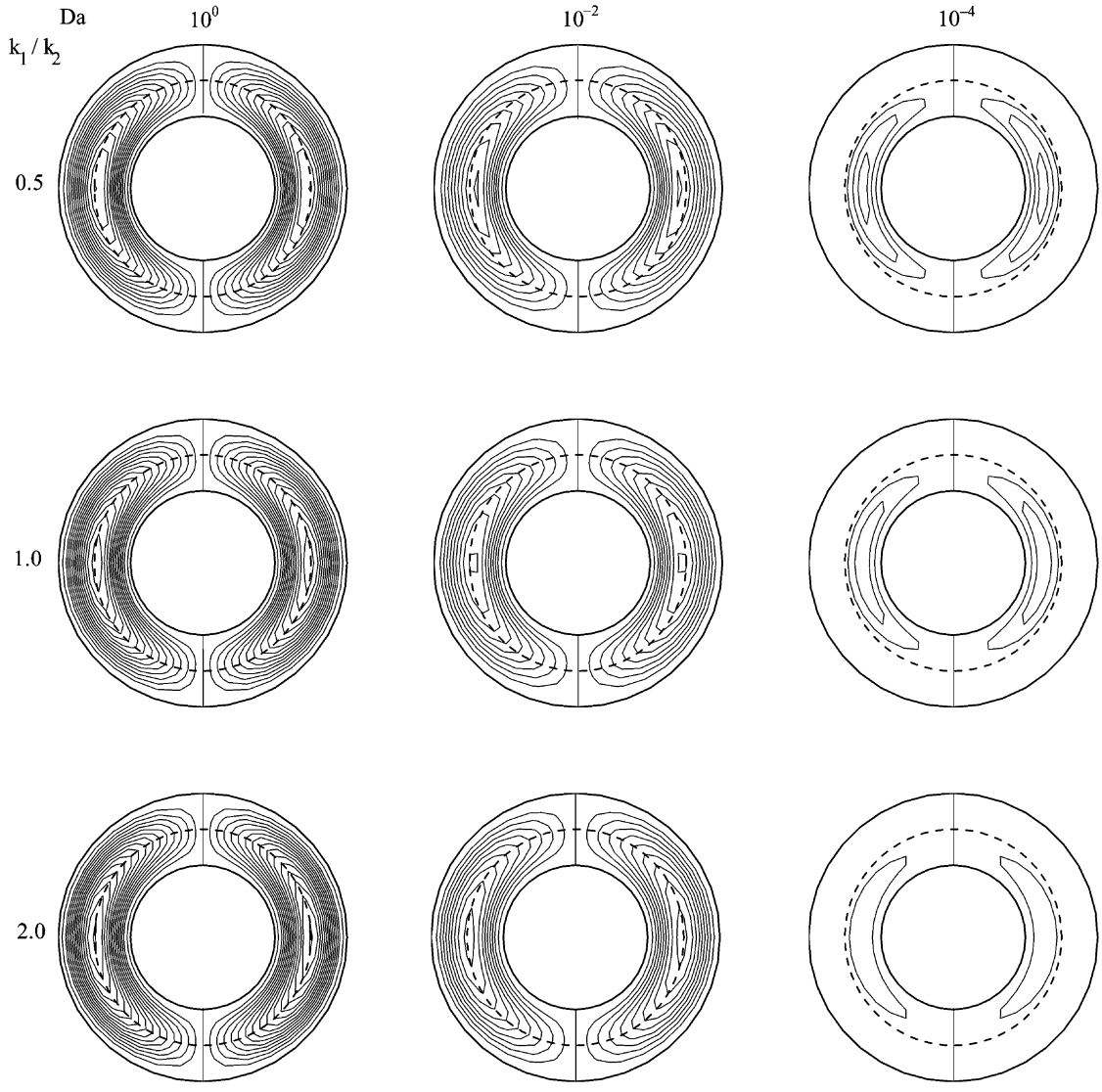

Fig. 5. Flow fields in a concentric annulus with a porous sleeve for $b = 1.50$, $Pr = 2 \times 10^4$, and $Ra = 0.1$ ($\Delta\Psi = 2.5 \times 10^{-6}$ for $Da = 10^{-4}$, and $\Delta\Psi = 5.0 \times 10^{-6}$ otherwise).

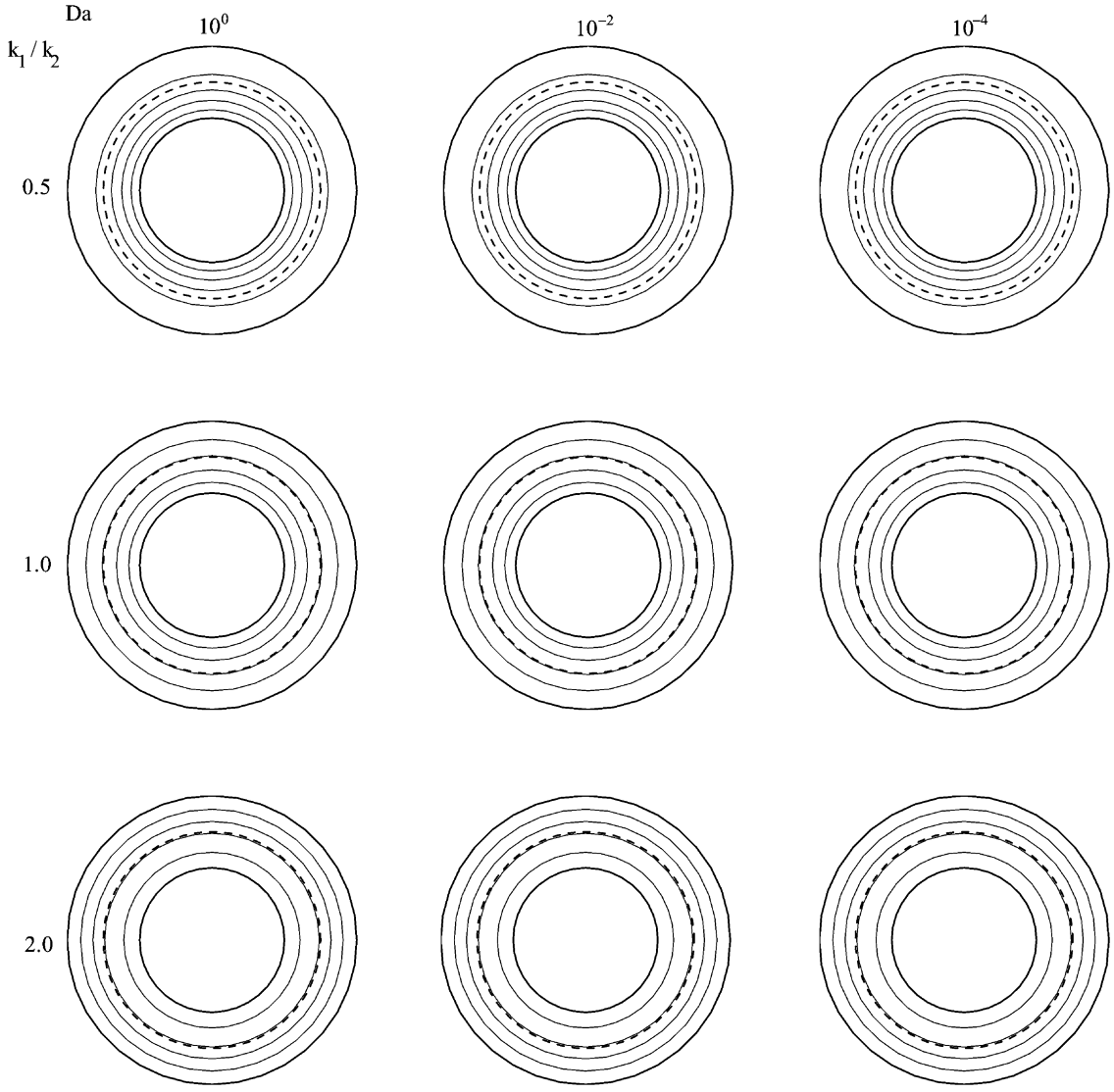

Fig. 6. Temperature fields in a concentric annulus with a porous sleeve for $b = 1.50$, $Pr = 2 \times 10^4$, and $Ra = 0.1$ ($\Delta\Theta = 0.2$).

For a given conductivity ratio, it appears that the temperature field is independent of the Darcy number (Fig. 6). When $k_1/k_2 = 1.0$, there is no distinction between the fluid and porous layers as far as heat transfer is concerned. For $k_1/k_2 < 1$, the porous sleeve is more conductive than the fluid layer. For this reason, the porous sleeve is almost uniform in temperature. On the other hand, for $k_1/k_2 > 1$, the temperature in the fluid layer is more uniform than that in the porous sleeve. Unlike the flow fields, the temperature fields for $Da = 10^0$ depend heavily on k_1/k_2. Although there is almost no flow resistance in the porous sleeve for $Da = 10^0$, the presence of a porous sleeve can promote ($k_1/k_2 > 1.0$) or demote ($k_1/k_2 < 1.0$) the heat flow. For low Rayleigh numbers, heat conduction is the dominant heat transfer mechanism. The Darcy number, although dictates the flow structure, has very little effect on the temperature field. The dependence of the temperature field on the Darcy number is expected to become important for highly convective flows that occur at high Rayleigh numbers.

The combined effects of porous sleeve thickness and conductivity ratio on the heat transfer results can be examined from Fig. 7, where average Nusselt numbers on the inner and outer cylinders are presented. It is observed that the average Nusselt number for the inner cylinder is always twice as large as that of the outer cylinders. However, if one takes into account the difference in the surface area, the average Nusselt numbers turn out to be the same because the radius of the outer cylinder is two times of that of the inner cylinder. This shows that energy is balanced between the inner and outer cylinders.

Also observed is that the average Nusselt numbers decreases monotonously with k_1/k_2. As one recalls from Fig. 3, an increase in the thermal conductivity ratio k_1/k_2 demotes convection in the fluid layer and thus reduces the overall heat transfer from the annulus. On the other

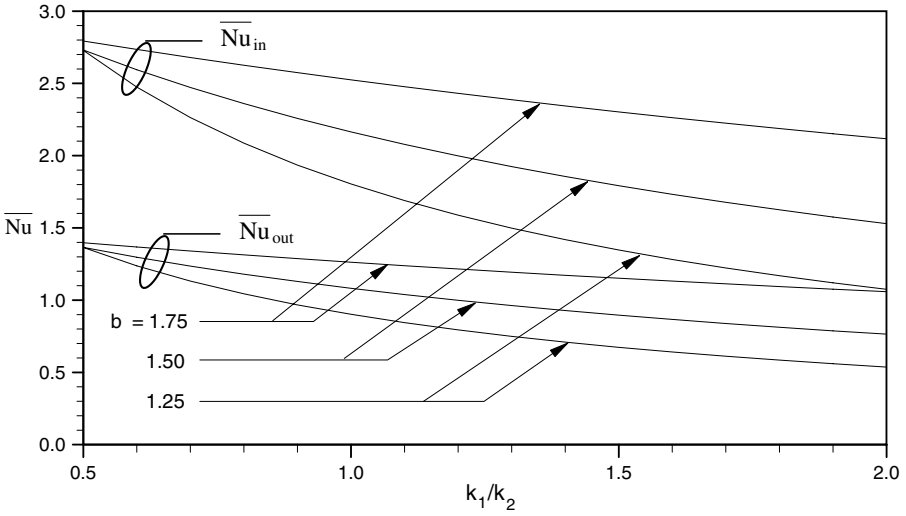

Fig. 7. Average Nusselt numbers on the inner and outer cylinders for various values of b and k_1/k_2 ($Da = 10^{-4}$ and $Ra = 0.1$).

hand, it is observed that the average Nusselt number increases with an increasing value of b. In other words, the thinner the porous sleeve, the better the heat transfer result. As one may recall from Fig. 2, a thinner porous sleeve allows a stronger convective flow to be developed in the fluid layer and which leads to an increase in the overall heat transfer. It is interesting to note that the average Nusselt numbers for $b = 1.25$ and 1.5 become identical at $k_1/k_2 = 0.5$. Based on this observation, one may expect that for a smaller thermal conductivity ratio k_1/k_2, the average Nusselt numbers for all three values of b would be the same.

5. Conclusions

A theoretical study was performed using the regular perturbation method and finite Fourier transform. The results show that two convective cells are induced by the differential heating between the inner and outer cylinders. The strength of these cells increases with the Rayleigh number. Also found is that the Prandtl number has an insignificant effect on the flow and temperature fields when the Rayleigh number is small.

The thinner a porous sleeve, the greater the strength of a convective cell. For a sufficiently thin porous sleeve, the porous sleeve behaves as if it were impermeable. At low Rayleigh numbers, the heat removal from the inner cylinder is mainly by conduction. However, at a higher Rayleigh number when heat convection becomes more important, it is expected that the porous sleeve thickness will play a much more important role in heat transfer. As the pore size in the porous sleeve decreases (i.e., the Darcy number decreases), the flow strength weakens. If the Darcy number is of the order of unity, the presence of the porous sleeve is negligible because its pore size is of the same order of magnitude as the gap width. Since conduction is the dominant heat transfer mode for the present study, thermal conductivity ratio k_1/k_2 does not significantly affect the flow field. Instead, it has a profound effect on the temperature distribution. For a given porous sleeve thickness, the temperature gradient in the fluid layer decreases with k_1/k_2 but it increases in the porous sleeve. Consequently, for a typical porous bearing ($Da < 10^{-4}$), an increase in the thermal conductivity ratio weakens the convective cells. Also, the effects of thermal conductivity ratio on the temperature gradients lead to a reduction of the average Nusselt numbers with k_1/k_2. Other than the thermal conductivity ratio, a thinner porous sleeve will also lead to a larger average Nusselt number.

While the present study has explored a fundamental problem in heat transfer, the analytical results obtained are not only useful for code validation, but also have important implications for practical applications. For example, the Darcy number associated with porous bearings is normally on the order of 10^{-8} to 10^{-9} and the thermal conductivity ratio is usually on the order of 10^{-3}. Based on the present results, one would expect a larger temperature gradient to occur in the fluid layer rather than the porous sleeve. In addition, heat dissipation by pure conduction through porous sleeve may be effective in operation.

Appendix A

$$A_{11} = -B_{11} + I_1(\gamma)A_{21} + K_1(\gamma)B_{21} + \Gamma_{21}, \tag{A1}$$

$$A_{12} = -(13/216)X_1 + X_2/18 - X_3/12 + 0.25X_8 - B_{22} + I_2(\gamma)A_{22} + K_2(\gamma)B_{22}, \tag{A2}$$

$$A_{21} = [-a_{\Gamma 1}(2b_{B21} + b_{B11}c_{B21}) + b_{\Gamma 1}(a_{B11}c_{B21} + 2a_{B21}) + c_{\Gamma 1}(a_{B21}b_{B11} - a_{B11}b_{B21})]/d_1, \tag{A3}$$

$$A_{22} = [-a_{k3}(4b_{B22} + b_{B12}c_{B22}) + b_{k3}(a_{B12}c_{B22} + 4a_{B22}) + c_{k3}(a_{B22}b_{B12} - a_{B12}b_{B22})]/d_3, \tag{A4}$$

$$B_{11} = [a_{\Gamma 1}(b_{A21}c_{B21} - b_{B21}c_{A21}) + b_{\Gamma 1}(a_{B21}c_{A21} - a_{A21}c_{B21}) + c_{\Gamma 1}(a_{A21}b_{B21} - a_{B21}b_{A21})]/d_1, \tag{A5}$$

$$B_{12} = [a_{k3}(b_{A22}c_{B22} - b_{B22}c_{A22}) + b_{k3}(a_{B22}c_{A22} - a_{A22}c_{B22}) + c_{k3}(a_{A22}b_{B22} - a_{B22}b_{A22})]/d_3, \quad \text{(A6)}$$

$$B_{21} = [a_{\Gamma 1}(b_{B11}c_{A21} - 2b_{A21}) - b_{\Gamma 1}(2a_{A21} - a_{B11}c_{A21}) + c_{\Gamma 1}(a_{B11}b_{A21} - a_{A21}b_{B11})]/d_1, \quad \text{(A7)}$$

$$B_{22} = [a_{k3}(b_{B12}c_{A22} + 4b_{A22}) - b_{k3}(4a_{A22} + a_{B12}c_{A22}) + c_{k3}(a_{B12}b_{A22} - a_{A22}b_{B12})]/d_3, \quad \text{(A8)}$$

$$C_{11} = -0.25(a/b)^2 A_{11,1} - [0.5\ln(a/b) + 0.25]B_{11,1} - (a/b)^2(0.25\ln(a/b) - 0.125)\Gamma_{11}, \quad \text{(A9)}$$

$$C_{12} = 0.125[-(a/b)^2 A_{12} + (b/a)^2(B_{12} - 4k_1 - 2(a/b)k_2)], \quad \text{(A10)}$$

$$C_{21} = -0.5\gamma^{-1}I_0(\gamma c/b)A_{21} + 0.5\gamma^{-1}K_0(\gamma c/b)B_{21} - (0.5\ln(c/b) + 0.25)\Gamma_{21}, \quad \text{(A11)}$$

$$C_{22} = k_{AC}A_{22} + k_{BC}B_{22} + k_{CC}, \quad \text{(A12)}$$

$$D_{11} = 0.125(a/b)^4 A_{11} + 0.25(a/b)^2 B_{11} + (a/b)^4(0.125\ln(a/b) - 0.03125)\Gamma_{11}, \quad \text{(A13)}$$

$$D_{12} = (a/b)^6/24A_{12} + 0.5(a/b)^2 \times (0.25B_{12} - k_1 + 0.5(a/b)k_2), \quad \text{(A14)}$$

$$D_{21} = [0.5(c/b)^2\gamma^{-1}I_0(\gamma c/b) - (c/b)\gamma^{-2}I_1(\gamma c/b)]A_{21} - [0.5(c/b)^2\gamma^{-1}K_0(\gamma c/b) + (c/b)\gamma^{-2}K_1(\gamma c/b)]B_{21} + 0.25(c/b)^2\Gamma_{21}, \quad \text{(A15)}$$

$$D_{22} = k_{AD}A_{22} + k_{BD}B_{22} + k_{CD}, \quad \text{(A16)}$$

$$E_{11} = -F_{11} + (k_1/k_2)^2(E_{21} + F_{21}) - (1/64)A'_{11} + (3/128)\Gamma'_{11}, \quad \text{(A17)}$$

$$E_{21} = \{-2a_{\Gamma 2}(b/c) + b_{\Gamma 2}[((k_1/k_2)^2 - 1)(a/b) + ((k_1/k_2)^2 + 1)(b/a)] + c_{\Gamma 2}(a^2 - b^2)/ac\}/d_2, \quad \text{(A18)}$$

$$F_{11} = \{a_{\Gamma 2}[(c/b)((k_1/k_2)^2 + 1) - ((k_1/k_2)^2 - 1)/(c/b)] - 2b_{\Gamma 2}(k_1/k_2)^2(a/b) - c_{\Gamma 2}(k_1/k_2)^2(a/c) \times [(c/b)^2 - 1]\}/d_2, \quad \text{(A19)}$$

$$F_{21} = \{2a_{\Gamma 2}(c/b)b_{\Gamma 2}[((k_1/k_2)^2 + 1)(a/b) + ((k_1/k_2)^2 - 1)(b/a)] - c_{\Gamma 2}[(a/b)^2 - 1](c/a)\}/d_2, \quad \text{(A20)}$$

$$G(\xi) = K_2(\gamma\xi)\int_1^\xi \zeta\bar{Z}(\zeta)I_2(\gamma\zeta)\mathrm{d}\zeta - I_2(\gamma\xi)\int_1^\xi \zeta\bar{Z}(\zeta)K_2(\gamma\zeta)\mathrm{d}\zeta, \quad \text{(A21)}$$

$$W(R) = \left(A_{22} - \int_1^R \xi Z(\xi)K_2(\gamma\xi)\mathrm{d}\xi\right)I_2(\gamma R) + \left(B_{22} + \int_1^R \xi Z(\xi)I_2(\gamma\xi)\mathrm{d}\xi\right)K_2(\gamma R), \quad \text{(A22)}$$

$$X_1 = 0.25\Gamma_{11}\Gamma'_{11}/Pr, \quad \text{(A23)}$$

$$X_2 = (0.25(A_{11}\Gamma'_{11} + A'_{11}\Gamma_{11}) - 0.1875\Gamma_{11}\Gamma'_{11})/Pr - q(3\sin\theta\Gamma'_{11} - \cos\theta\Gamma_{11})/64, \quad \text{(A24)}$$

$$X_3 = \left[0.25A_{11}A'_{11} + 0.09375\left(A_{11}\Gamma'_{11} - 3A'_{11}\Gamma_{11} + \Gamma_{11}\Gamma'_{11}\right)\right]/Pr + q\left[\sin\theta\left(-6A'_{11} + 16B'_{11} + 7\Gamma'_{11}\right)/128 + \cos\theta(2A_{11} - 3\Gamma_{11})/128\right], \quad \text{(A25)}$$

$$X_4 = 0.5(B_{11}\Gamma'_{11} - B'_{11}\Gamma_{11})/Pr - 0.125q(\sin\theta B'_{11} - \cos\theta B_{11}), \quad \text{(A26)}$$

$$X_5 = \left[0.5\left(-A_{11}B'_{11} + A'_{11}B_{11}\right) + 0.125\left(5B_{11}\Gamma'_{11} - B'_{11}\Gamma_{11}\right) + C_{11}\Gamma'_{11} - C'_{11}\Gamma_{11}\right]/Pr - q[\sin\theta(0.125B'_{11} + 0.5C'_{11}) + \cos\theta(0.125B_{11} - 0.5C_{11})], \quad \text{(A27)}$$

$$X_6 = [(3A_{11}B'_{11} + 5A'_{11}B_{11})/8 - A_{11}C'_{11} + A'_{11}C_{11} - (3B_{11}\Gamma'_{11} + 5B'_{11}\Gamma_{11})/32 - C'_{11}\Gamma_{11}]/Pr - q[\sin\theta(0.5C'_{11} + E_{11}) + \cos\theta E'_{11}], \quad \text{(A28)}$$

$$X_7 = (B_{11}B'_{11} - D_{11}\Gamma'_{11} - D'_{11}\Gamma_{11})/Pr - 0.5q(\sin\theta D'_{11} + \cos\theta D_{11}), \quad \text{(A29)}$$

$$X_8 = \left(-A_{11}D'_{11} - A'_{11}D_{11} + 0.5B_{11}B'_{11} + B_{11}C'_{11} + B'_{11}C_{11} - D'_{11}\Gamma_{11}\right)/Pr + q\left[\sin\theta\left(0.5D'_{11} + F_{11}\right) - \cos\theta F'_{11}\right], \quad \text{(A30)}$$

$$X_9 = (B_{11}D'_{11} - B'_{11}D_{11})/Pr, \quad \text{(A31)}$$

$$Y_1 = q(k_1/k_2)\gamma^{-3}(-\sin\theta A'_{21} + \cos\theta A_{21}), \quad \text{(A32)}$$

$$Y_2 = q(k_1/k_2)\gamma^{-3}(\sin\theta B'_{21} - \cos\theta B_{21}), \quad \text{(A33)}$$

$$Y_3 = 0.125q(k_1/k_2)(-\sin\theta\Gamma'_{21} + \cos\theta\Gamma_{21}), \quad \text{(A34)}$$

$$Y_4 = -0.5\gamma A_{21}\Gamma'_{21}, \quad \text{(A35)}$$

$$Y_5 = -0.5\gamma B_{21}\Gamma'_{21}, \quad \text{(A36)}$$

$$Y_6 = -q(k_1/k_2)[\sin\theta(0.5C'_{21} + 0.125\Gamma'_{21}) + \cos\theta(-0.5C_{21} + 0.125\Gamma_{21})], \quad \text{(A37)}$$

$$Y_7 = -\gamma A_{21}C'_{21}, \quad \text{(A38)}$$

$$Y_8 = \gamma B_{21}C'_{21}, \quad \text{(A39)}$$

$$Y_9 = -q(k_1/k_2)[\sin\theta(0.5C'_{21} + E_{21} - 0.125\Gamma'_{21}) + \cos\theta E'_{21}], \quad \text{(A40)}$$

$$Y_{10} = 0.5(A_{21}\Gamma'_{21} + A'_{21}\Gamma_{21}), \quad \text{(A41)}$$

$$Y_{11} = 0.5(B_{21}\Gamma'_{21} + B'_{21}\Gamma_{21}), \quad \text{(A42)}$$

$$Y_{12} = A_{21}C'_{21} + A'_{21}(C_{21} + 0.5\Gamma_{21}), \quad \text{(A43)}$$

$$Y_{13} = B_{21}C'_{21} + B'_{21}(C_{21} + 0.5\Gamma_{21}), \quad \text{(A44)}$$

$$Y_{14} = \Gamma_{21}\Gamma'_{21} - 0.5q(k_1/k_2)(\sin\theta D'_{21} + \cos\theta D_{21}), \quad \text{(A45)}$$

$$Y_{15} = A_{21}(-\gamma D'_{21} + \gamma^{-1}\Gamma'_{21}) - q(k_1/k_2)\gamma^{-3}\sin(\theta)A'_{21}, \quad \text{(A46)}$$

$$Y_{16} = B_{21}(\gamma D'_{21} - \gamma^{-1}\Gamma'_{21}) + q(k_1/k_2)\gamma^{-3}\sin(\theta)B'_{21}, \quad \text{(A47)}$$

$$Y_{17} = q(k_1/k_2)[\sin\theta(0.5D'_{21} + F_{21}) - \cos\theta F'_{21}], \quad \text{(A48)}$$

$$Y_{18} = A_{21}(D'_{21} - \gamma^{-2}\Gamma'_{21}) - A'_{21}(D_{21} - \gamma^{-2}\Gamma_{21}), \quad \text{(A49)}$$

$$Y_{19} = B_{21}(D'_{21} - \gamma^{-2}\Gamma'_{21}) - B'_{21}(D_{21} - \gamma^{-2}\Gamma_{21}), \quad \text{(A50)}$$

$$Y_{20} = -D_{21}\Gamma'_{21} + D'_{21}\Gamma_{21}, \quad \text{(A51)}$$

$$Z(R) = Y_1\int_1^R \xi^{-3}I_0(\gamma\xi)\mathrm{d}\xi + Y_2\int_1^R \xi^{-3}K_0(\gamma\xi)\mathrm{d}\xi + Y_3\ln(R)^2 + [Y_4I_0(\gamma R) + Y_5K_0(\gamma R) + Y_6]\ln(R) + Y_7I_0(\gamma R) + Y_8K_0(\gamma R) + Y_9 + \{[Y_{10}I_1(\gamma R) + Y_{11}K_1(\gamma R)]\ln(R) + Y_{12}I_1(\gamma R) + Y_{13}K_1(\gamma R)\}R^{-1} + \{Y_{14}\ln(R) + Y_{15}I_0(\gamma R) + Y_{16}K_0(\gamma R) + Y_{17}\}R^{-2} + \{Y_{18}I_1(\gamma R) + Y_{19}K_1(\gamma R)\}R^{-3} + Y_{20}R^{-4}, \quad \text{(A52)}$$

$$\Gamma_{11} = -0.5q\sin\theta, \tag{A53}$$

$$\Gamma_{21} = (k_1/k_2)q\gamma^{-2}\sin\theta, \tag{A54}$$

$$\begin{aligned} a_{A21} = {} & -\gamma^{-1}I_0(\gamma) + [\gamma^{-2} + 0.375 - 0.25(a/b)^2 \\ & - 0.125(a/b)^4]I_1(\gamma) + 0.5\gamma^{-1}[1 + (c/b)^2]I_0(\gamma c/b) \\ & - (c/b)\gamma^{-2}I_1(\gamma c/b), \end{aligned} \tag{A55}$$

$$a_{A22} = [(a/b)^6/24 - 0.125(a/b)^2 + 1/12]I_2(\gamma) - k_{AC} - k_{AD}, \tag{A56}$$

$$a_{B11} = -0.5\ln(a/b) + 0.125[(a/b)^4 - 1], \tag{A57}$$

$$a_{B12} = -(a/b)^6/24 + 0.25(a/b)^2 - 1/3 + 0.125(b/a)^2, \tag{A58}$$

$$\begin{aligned} a_{B21} = {} & \gamma^{-1}K_0(\gamma) + [\gamma^{-2} + 0.375 - 0.25(a/b)^2 \\ & - 0.125(a/b)^4]K_1(\gamma) - 0.5\gamma^{-1}[1 + (c/b)^2]K_0(\gamma c/b) \\ & - (c/b)\gamma^{-2}K_1(\gamma c/b), \end{aligned} \tag{A59}$$

$$a_{B22} = [(a/b)^6/24 - 0.125(a/b)^2 + 1/12] \times K_2(\gamma) - k_{BC} - k_{BD}, \tag{A60}$$

$$\begin{aligned} a_{k3} = {} & [-(13/5184)(a/b)^6 + (13/1728)(a/b)^2 \\ & - (419/331776)]X_1 + ((a/b)^6/432 \\ & - (a/b)^2/144 + (53/27648))X_2 \\ & + (-(a/b)^6/288 + (a/b)^2/96 - (5/1152))X_3 \\ & - (137/10368)X_4 + (19/1728)X_5 - X_6/72 \\ & + ((a/b)^6/96 - (a/b)^2/32 + 5/48)X_8 \\ & - 0.5((a/b)^2 + (b/a)^2)k_1 + 0.25((a/b)^3 - (b/a))k_2 \\ & - k_{CC} - k_{CD}, \end{aligned} \tag{A61}$$

$$\begin{aligned} a_{\Gamma 1} = {} & \{0.125(a/b)^4[-\ln(a/b) + 0.25] + 0.25(a/b)^2 \\ & \times [-\ln(a/b)0.5] - 0.15625\}\Gamma_{11} \\ & + [0.125 - 0.125(a/b)^4 + 0.5\ln(c/b) \\ & + 0.25(c/b)^2]\Gamma_{21}, \end{aligned} \tag{A62}$$

$$\begin{aligned} a_{\Gamma 2} = {} & [(a/b)^3 - (a/b)]/64A'_{11} + 0.125(a/b) \\ & \times [\ln(a/b)^2 - \ln(a/b)]B'_{11} + 0.5(a/b)\ln(a/b)C'_{11} \\ & - 0.25(a/b)^2 - 0.5(b/a)\ln(a/b)D'_{11} \\ & + [(3/128)(a/b) + (a/b)^3/64(\ln(a/b) - 1.5)]\Gamma'_{11}, \end{aligned} \tag{A63}$$

$$\begin{aligned} b_{A21} = {} & [0.125 - 0.25(a/b)^2 + 0.125(a/b)^4 - \gamma^{-2}]I_1(\gamma) \\ & + 0.5[1 - (c/b)^2]\gamma^{-1}I_0(\gamma c/b) + (c/b)\gamma^{-2}I_1(\gamma c/b), \end{aligned} \tag{A64}$$

$$\begin{aligned} b_{A22} = {} & [-(a/b)^6/12 - 0.25(a/b)^2 + (1/3)]I_2(\gamma) \\ & - 2k_{AC} + 2k_{AD}, \end{aligned} \tag{A65}$$

$$b_{B11} = -0.5\ln(a/b) - 0.375 + 0.5(a/b)^2 - 0.125(a/b)^4, \tag{A66}$$

$$b_{B12} = (a/b)^6/12 - (1/3) + 0.25(b/a)^2, \tag{A67}$$

$$\begin{aligned} b_{B21} = {} & [0.125 - 0.25(a/b)^2 + 0.125(a/b)^4 - \gamma^{-2}]K_1(\gamma) \\ & - 0.5[1 - (c/b)^2]\gamma^{-1}K_0(\gamma c/b) + (c/b)\gamma^{-2}K_1(\gamma c/b), \end{aligned} \tag{A68}$$

$$\begin{aligned} b_{B22} = {} & [-(a/b)^6/12 - .25(a/b)^2 + (1/3)]K_2(\gamma) \\ & - 2k_{BC} + 2k_{BD}, \end{aligned} \tag{A69}$$

$$\begin{aligned} b_{k3} = {} & [-(13/2592)(a/b)^6 + (13/864)(a/b)^2 \\ & - (419/165888)]X_1 + (-(a/b)^6/216 \\ & - (a/b)^2/72 + (67/13824))X_2 \\ & + ((a/b)^6/144 + (a/b)^2/48 - (7/576))X_3 \\ & - (293/10368)X_4 + (43/1728)X_5 \\ & - (5/144)X_6 + (-(a/b)^6/48 - (a/b)^2/16 \\ & + (1/48))X_8 + X_9/16 + ((a/b)^2 \\ & - (b/a)^2)k_1 - 0.5((a/b)^3 + (b/a))k_2 \\ & - 2k_{CC} + 2k_{CD}, \end{aligned} \tag{A70}$$

$$\begin{aligned} b_{\Gamma 1} = {} & \{0.125(a/b)^4[\ln(a/b) - 0.25] - 0.25(a/b)^2[\ln(a/b) - 0.5] \\ & - 0.09375\}\Gamma_{11} + [0.375 - 0.25(a/b)^2 + 0.125(a/b)^4 \\ & + 0.5\ln(c/b) - 0.25(c/b)^2]\Gamma_{21}, \end{aligned} \tag{A71}$$

$$\begin{aligned} b_{\Gamma 2} = {} & \gamma^{-3}(c/b)\left[A'_{21}\int_1^{c/b}\xi^{-3}I_0(\gamma\xi)\mathrm{d}\xi - B'_{21}\int_1^{c/b}\xi^{-3}K_0(\gamma\xi)\mathrm{d}\xi\right] \\ & + 0.5(c/b)\ln(c/b)C'_{21} - 0.5(b/c)\ln(c/b)D'_{21} \\ & + 0.125(c/b)[\ln(c/b)^2 - \ln(c/b)]\Gamma'_{21}, \end{aligned} \tag{A72}$$

$$c_{A21} = I_1(\gamma) - 0.5[1 + (c/b)^2]\gamma I_0(\gamma c/b) + (c/b)I_1(\gamma c/b), \tag{A73}$$

$$c_{A22} = 4I_2(\gamma) - \gamma I_1(\gamma) + 2\gamma^2 k_{AC} - 2\gamma^2 k_{AD}, \tag{A74}$$

$$c_{B21} = K_1(\gamma) + 0.5[1 + (c/b)^2]\gamma K_0(\gamma c/b) + (c/b)K_1(\gamma c/b), \tag{A75}$$

$$c_{B22} = 4K_2(\gamma) + \gamma K_1(\gamma) + 2\gamma^2 k_{BC} - 2\gamma^2 k_{BD}, \tag{A76}$$

$$\begin{aligned} c_{k3} = {} & X_1/108 - X_2/36 + X_3/6 + X_4/32 - X_5/16 \\ & + 0.25(X_6 - X_7 + 2X_8 - X_9) + 2\gamma^2 k_{CC} - 2\gamma^2 k_{CD}, \end{aligned} \tag{A77}$$

$$c_{\Gamma 1} = \Gamma_{11} + (-0.5\ln(c/b)\gamma^2 + 2 + 0.25[1 - (c/b)^2]\gamma^2)\Gamma_{21}, \tag{A78}$$

$$\begin{aligned} c_{\Gamma 2} = {} & 0.03125A'_{11} - 0.125B'_{11} + 0.5C'_{11} - 0.5D'_{11} \\ & - 0.03125\Gamma'_{11} - \gamma^{-3}I_0(\gamma)A'_{21} + \gamma^{-3}K_0(\gamma)B'_{21} \\ & - 0.5C'_{21} + 0.5D'_{21} + 0.125\Gamma'_{21}, \end{aligned} \tag{A79}$$

$$\begin{aligned} d_1 = {} & a_{B11}(b_{B21}c_{A21} - b_{A21}c_{B21}) + a_{A21}(b_{B11}c_{B21} + 2b_{B21}) \\ & - A_{B21}(2b_{A21} + b_{B11}c_{A21}), \end{aligned} \tag{A80}$$

$$\begin{aligned} d_2 = {} & [(1 - (k_1/k_2)^2)(c/b) + (1 + (k_1/k_2)^2)(b/c)](a/b) \\ & - [(1 + (k_1/k_2)^2)(c/b) + (1 - (k_1/k_2)^2)(b/c)](b/a), \end{aligned} \tag{A81}$$

$$\begin{aligned} d_3 = {} & a_{B12}(b_{B22}c_{A22} - b_{A22}c_{B22}) + a_{A22}(b_{B12}c_{B22} + 4b_{B22}) \\ & - a_{B22}(4b_{A22} + b_{B12}c_{A22}), \end{aligned} \tag{A82}$$

$$k_1 = [X_1/384\ln(a/b)^2 + (-(25/4608)X_1 + X_2/384)\ln(a/b) + (415/110592)X_1 - (25/9216)X_2 + X_3/384](a/b)^6 + [(X_4/144)\ln(a/b)^3 + (-(11/576)X_4 + X_5/96) \times \ln(a/b)^2 + ((85/3456)X_4 - (11/576)X_5 + X_6/48) \times \ln(a/b) - (137/10368)X_4 + (19/1728)X_5 - X_6/72](a/b)^4 + [-(X_7/32)\ln(a/b)^2 + ((X_7/64) - (X_8/16))\ln(a/b)](a/b)^2 + (X_9/16)\ln(a/b), \quad \text{(A83)}$$

$$k_2 = [(X_1/64)\ln(a/b)^2 + (-(7/265)X_1 + X_2/64)\ln(a/b) + (35/2048)X_1 - (7/512)X_2 + X_3/64](a/b)^5 + (1 - (k_1/k_2)^2)(b/c)](b/a) + [X_4/36\ln(a/b)^3 + (-X_4/18 + X_5/24)\ln(a/b)^2 + ((13/216)X_4 - X_5/18 + X_6/12)\ln(a/b) - (293/10368)X_4 + (43/1728)X_5 - (5/144)X_6](a/b)^3 + \{-(X_7/16)\ln(a/b)^2 - (X_7/32 + X_8/8)\ln(a/b) + X_7/64 - X_8/16\}(a/b) + (X_9/16)(b/a), \quad \text{(A84)}$$

$$k_{AC} = -0.25\int_1^{c/b} \xi^{-1} I_2(\gamma\xi)\mathrm{d}\xi, \quad \text{(A85)}$$

$$k_{BC} = -0.25\int_1^{c/b} \xi^{-1} K_2(\gamma\xi)\mathrm{d}\xi, \quad \text{(A86)}$$

$$k_{CC} = -0.25\int_1^{c/b} \xi^{-1} G(\xi)\mathrm{d}\xi, \quad \text{(A87)}$$

$$k_{AD} = 0.25\int_1^{c/b} \xi^{3} I_2(\gamma\xi)\mathrm{d}\xi, \quad \text{(A88)}$$

$$k_{BD} = 0.25\int_1^{c/b} \xi^{3} K_2(\gamma\xi)\mathrm{d}\xi, \quad \text{(A89)}$$

$$k_{CD} = -0.25\int_1^{c/b} \xi^{3} G(\xi)\mathrm{d}\xi, \quad \text{(A90)}$$

$$q = [(k_1/k_2)\ln(c/b) - \ln(a/b)]^{-1}, \quad \text{(A91)}$$

$$\gamma = 1/\sqrt{Da}. \quad \text{(A92)}$$

References

[1] E.H. Bishop, C.T. Carley, Photographic studies of natural convection between concentric cylinders, in: Proceedings of the 1966 Heat Transfer and Fluid Mechanics Institute, Stanford University Press, 1966, pp. 63–78.

[2] R.E. Powe, C.T. Carley, E.H. Bishop, Free convective flow patterns in cylindrical annuli, J. Heat Transfer 91 (3) (1969) 310–314.

[3] R.E. Powe, C.T. Carley, S.L. Carruth, A numerical solution for natural convection in cylindrical annuli, J. Heat Transfer 93 (2) (1971) 210–220.

[4] T.H. Kuehn, R.J. Goldstein, An experimental and theoretical study of natural convection in the annulus between horizontal concentric cylinders, J. Fluid Mech. 74 (1976) 695–719.

[5] T.H. Kuehn, R.J. Goldstein, A parametric study of Prandtl number and diameter ratio effects on natural convection heat transfer in horizontal cylindrical annuli, J. Heat Transfer 102 (1980) 768–770.

[6] M.C. Charrier-Mojtabi, A. Mojtabi, J.P. Caltagirone, Numerical solution of a flow due to natural convection in horizontal cylindrical annulus, J. Heat Transfer 101 (1979) 171–173.

[7] L.S. Yao, Analysis of heat transfer in slightly eccentric annuli, J. Heat Transfer 102 (1980) 279–284.

[8] G. Guj, F. Stella, Natural convection in horizontal eccentric annuli: numerical study, Numer. Heat Transfer, Part A: Appl. 27 (1) (1995) 89–105.

[9] C.-H. Cheng, C.-C. Chao, Numerical prediction of the buoyancy-driven flow in the annulus between horizontal eccentric elliptical cylinders, Numer. Heat Transfer, Part A: Appl. 30 (3) (1996) 283–303.

[10] C. Shu, K.S. Yeo, Q. Yao, An efficient approach to simulate natural convection in arbitrary eccentric annuli by vorticity-stream function formulation, Numer. Heat Transfer, Part A: Appl. 38 (7) (2000) 739–756.

[11] F. Shahraki, Modeling of buoyancy-driven flow and heat transfer for air in a horizontal annulus: effects of vertical eccentricity and temperature-dependent properties, Numer. Heat Transfer, Part A: Appl. 42 (6) (2002) 603–621.

[12] J.P. Caltagirone, Thermoconvective instabilities in a porous medium bounded by two concentric horizontal cylinders, J. Fluid Mech. 76 (2) (1976) 337–362.

[13] H.H. Bau, Low Rayleigh number thermal convection in a saturated porous medium bounded by two horizontal, eccentric cylinders, J. Heat Transfer 106 (1) (1984) 166–175.

[14] S. Ishizawa, E. Hori, The flow of a viscous fluid through a porous wall into a narrow gap, Bull. JSME 9 (36) (1966) 719–730.

[15] J.C. Leong, F.C. Lai, Mixed convection in rotating concentric annulus with a porous sleeve, in: Proceedings of the 2003 ASME National Heat Transfer Conference, HT2003-47288 (CD-ROM).

[16] J.C. Leong, Heat transfer and fluid flow in rotating cylinders with a porous sleeve, PhD Dissertation, University of Oklahoma, Norman, OK, 2002.

[17] M.N. Ozisik, Boundary Value Problems of Heat Conduction, International Textbook Company, Pennsylvania, 1968.

[18] L.R. Mack, E.H. Bishop, Natural convection between horizontal concentric cylinders for low Rayleigh numbers, Quart. J. Mech. Appl. Math. 21 (1968) 223–241.

[19] J. Huetz, J.P. Petit, Natural and mixed convection in concentric annular spaces – experimental and theoretical results for liquid metals, in: Proceedings of the 5th International Heat Transfer Conference, vol. 3, 1974, pp. 169–172.

[20] J.R. Custer, E.J. Shaughnessy, Thermoconvective motion of low Prandtl number fluids within a horizontal cylindrical annulus, J. Heat Transfer 99 (4) (1977) 596–602.